Fol. 41 B

International Council for the
Exploration of the Sea

ICES C.M. 1994/B:40
Fish Capture Committee
Ref. D + L

COINCIDENCE ECHO STATISTICS

by

Kenneth G. Foote
Institute of Marine Research
5024 Bergen, Norway

ABSTRACT

Two scatterers at similar range give an echo which may appear to be due to a single scatterer. Methods for determining target strength that depend on resolving single scatterers may fail in this instance. Statistics associated with the described special case of coincidence are derived and illustrated by theoretical computation for the SIMRAD ES38B split-beam transducer with 38-kHz operating frequency.

RESUME: STATISTIQUES D'ECHOES CONFONDUS

Deux diffuseurs à une même distance produisent un écho qui peut apparaître comme être dû à un seul. Les méthodes pour déterminer les index de réflexion dependant de l'angle de résolution des diffuseurs peut s'avérer inopérante dans ce cas précis. Des statistiques dans le cas spécial de coïncidence sont établies et illustrées par un calcul théorique pour le sondeur SIMRAD ES38B à faisceau scindé traivaillant sur 38 kHz.

INTRODUCTION

Many methods used to measure fish target strength in situ depend on resolution of single target echoes. These include, for example, indirect methods, in which the effect of beam pattern is removed statistically (Foote 1991), and direct methods, for example, those of dual beams and split beams, in which the beam pattern effect is removed by means of phase measurement with multiple beams (Ehrenberg 1979).

It is generally appreciated that single-target selection criteria must be used with care, if not great care, to avoid effects due to the presence of multiple targets at similar ranges. A practical illustration of the effect of selection criteria on the resultant target strength distribution is obtained by changing the acceptance limits for echo length. Increasing the upper limit often increases the registration of large targets, while that of decreasing the same may radically decrease both the number and magnitude of accepted echoes. This illustration becomes vivid when fish are loosely concentrated, as during the process of night-time dispersion. Dual-beam or split-beam echo sounding systems, with so-called target strength analyzers, generally continue to deliver target strength data whatever the state of concentration.

The interesting question thus arises as to the effect of multiple targets with coincident echoes on the apparent single-target target strength distribution. This question is addressed here, for definiteness, with respect to the target strength analyzer in a particular split-beam echo sounder system, that of the SIMRAD EK500 echo sounder (Bodholt et al. 1989).

THEORY

Beam pattern of a transducer aperture

The transducer is defined as a shaded planar array of identical square elements. A subset of the elements defines an aperture. For the particular aperture A, the beam pattern amplitude factor in the direction $\hat{k}$ is

$$D_A(\hat{k}) = \sum_{j \varepsilon A} w_j \int_A \exp(i\underline{k}\cdot\underline{r})\, dA_j \;/\; \sum_{j' \varepsilon A} w_{j'} \qquad (1)$$

where $\underline{k}$ is the wavevector, $\hat{k}=k/k$, w_j is the amplitude weight of the j-th transducer element, and $\underline{r}$ is the position of the differential surface element dA_j. In rectangular coordinates, $k=(\sin\theta\cos\phi,\ \sin\theta\sin\phi,\ \cos\theta)$. Referring $\underline{r}$ to the center $\underline{r}_j$ of the j-th transducer element, and integrating over the area,

$$D_A(\hat{k}) = D_1(\hat{k}) \sum_{j \varepsilon A} w_j \exp(i\underline{k}\cdot\underline{r}_j) \;/\; \sum_{j' \varepsilon A} w_{j'} \quad , \qquad (2)$$

where $D_1=\mathrm{sinc}(ka\sin\theta\cos\phi)\,\mathrm{sinc}(ka\sin\theta\sin\phi)$ is the beam pattern amplitude factor of a single, square array element of side length a, $\mathrm{sinc}(x)=\sin(x)/x$.

Echo amplitude due to multiple targets at similar range

The echo amplitude is developed for the transducer farfield and for a range that is large compared to the transmit pulse length $c\tau$, where c is the speed of sound, and τ is the pulse duration:

$$p = \sum p_i\, s_i(t-2r_i/c) \quad , \qquad (3)$$

where p_i is the echo amplitude due to the i-th target, s_i is the corresponding echo signal waveform, and r_i is the range of the i-th target. For targets at similar range, and to within essentially the same constant of proportionality, $s_i = s$ for all i, and

$$p_i = b_i \sigma_i^{\frac{1}{2}} \quad , \tag{4}$$

where $b_i = D_{Ti} D_{Ri}$, D_{Ti} and D_{Ri} are the beam pattern amplitude factors of the respective transmit and receive apertures in the direction of the i-th target, and σ_i is the backscattering cross section of the same. If the transmit pulse is narrowband, hence with pulse duration that is large compared to the acoustic wavelength λ, and the ranges differ by no more than, say, one-half wavelength, then

$$p = \sum_i b_i \sigma_i^{\frac{1}{2}} \exp[(-1)^{\frac{1}{2}} \psi_i] \quad , \tag{5}$$

where ψ_i is the phase associated with the i-th target, namely $4\pi r_i \bmod \lambda$.

In the special case of just two targets, which is the one considered here, equation (5) can be simplified. To within a constant phase factor,

$$p = b_1 \sigma_1^{\frac{1}{2}} + b_2 \sigma_2^{\frac{1}{2}} \exp(i\chi) \quad , \tag{6}$$

where χ is the relative phase.

Split-beam echo processing

A split-beam transducer is electrically divided into quadrants. When transmitting, all quadrants are excited simultaneously, forming a single beam. When receiving, each quadrant acts independently to generate its own received echo signal. Half-beams are formed, and the phase difference between fore-and-aft halves and port-and-starboard halves detected. Knowing these two angles, hence target direction, the beam pattern is also known. The effect of the beam pattern on the sum-beam echo amplitude can thus be removed, resulting in an estimate for σ_i. A mathematical description follows.

For the general echo amplitude p,

$$p = |p| \exp\{i \tan^{-1}[\mathrm{Im}(p)/\mathrm{Re}(p)]\} \quad . \tag{7}$$

The phase is $\tan^{-1}[\mathrm{Im}(p)/\mathrm{Re}(p)]$. The quadrants of the transducer are numbered sequentially from the forward starboard quarter (1), to forward port (2), to aft port (3), to aft starboard (4). The result of combining the echo pressure registered by quadrants 1 and 2 is the half-beam h_{12}, and so forth. The angle of the target relative to the transducer in the fore-and-aft plane is

$$\alpha = S^{-1}\{\tan^{-1}[\mathrm{Im}(h_{12})/\mathrm{Re}(h_{12})] - \tan^{-1}[\mathrm{Im}(h_{34})/\mathrm{Re}(h_{34})]\} \quad , \tag{8}$$

where S is the so-called angle sensitivity factor, which is used to convert the phase difference to a spatial angle. The factor S is approximately equal to kd, where d is the effective distance between the transducer halves. The angle of the target in the port-and-starboard plane is

$$\beta = S^{-1}\{\tan^{-1}[\mathrm{Im}(h_{14})/\mathrm{Re}(h_{14})] - \tan^{-1}[\mathrm{Im}(h_{23})/\mathrm{Re}(h_{23})]\} \quad . \tag{9}$$

Equations (8) and (9) apply in the usual small-angle limit.

In a rectangular coordinate system with origin at the transducer center, x-axis pointing to starboard, y-axis forward, and z-axis downward,

$$\alpha = \hat{k}\cdot\hat{y} = \sin\theta\sin\phi \quad , \tag{10a}$$

$$\beta = \hat{k}\cdot\hat{x} = \sin\theta\cos\phi \quad , \tag{10b}$$

hence

$$\theta = \sin^{-1}(\alpha^2 + \beta^2)^{\frac{1}{2}} \quad , \tag{11a}$$

$$\phi = \tan^{-1}(\alpha/\beta) \quad . \tag{11b}$$

That is, the target position can be identified in ordinary polar coordinates based on measurement of half-beam phase differences, with immediate computation of α and β.

Two targets at similar range but generally different angular locations (θ_1,ϕ_1) and (θ_2,ϕ_2) will produce echoes that appear to be due to a single scatterer at a third location (θ,ϕ). If this lies in the main lobe of the split-beam transducer, it will, under the stated condition of similar range, be perceived as a single scatterer, and compensation for the apparent beam pattern loss accordingly applied. Larger apparent target angles are rejected. A series of measurements in the presence of multiple targets will thus in general produce a distribution of apparent single-target target strengths, at least some of which are spurious.

COMPUTATIONAL METHOD

In order to investigate the effect of multiple targets on the target strength distribution derived by means of split-beam processing, the two-target case is considered according to the following model.

Split-beam transducer For definiteness, this is assumed to be the SIMRAD ES38B transducer. This is a truncated square array of identical square elements of side length 30 mm and center-to-center distance along rows and columns of 32 mm, with operating frequency of 38 kHz. The amplitude weights in the forward starboard quadrant are shown in Fig. 1.

100	100	70		
100	100	70	70	
100	100	100	70	70
100	100	100	100	100
100	100	100	100	100

+

Fig. 1. Amplitude weights of elements in the forward starboard quadrant of the SIMRAD ES38B transducer.

<u>Transducer angle sensitivity factor</u> The nominal figure given by the manufacturer is 21.9 (Bodholt 1990). For the sound speed assumed here, namely 1470.6 m/s, defined by temperature $5^{\circ}C$, salinity 35 ppt, pH 8.8, and depth 0 m (Mackenzie 1981), this factor was determined by simulating the effect of a single target moved uniformly over the transducer beam cross section and requiring that the compensation not introduce a bias into the mean target strength. The resulting factor is thus S=23.2.

<u>Spatial distribution</u> The target range is assumed to be constant and equal for the two targets to within one-half the acoustic wavelength. The targets are assumed to be distributed with equal probability of occurrence anywhere in the cross section of the transducer beam within the -6-dB level, i.e., within the angular zone of acceptance for split-beam processing. For the ES38B transducer and medium sound speed of 1470.6 m/s, this limiting polar angle is to a fair approximation 4.66 deg.

<u>Target strength distributions</u> Each of two distributions is considered through the probability density function of target strength TS.

(1) Constant target strengths: The respective target strength distributions are

$$f_1(TS) = \delta(TS)$$

and

$$f_2(TS) = \delta(TS + \Delta TS) \quad ,$$

where δ is the Dirac delta function, and ΔTS is the constant difference in TS.

(2) Normally distributed target strengths: Both target strengths independently follow the same normal distribution, namely

$$f(TS) = (2\pi s^2)^{-\frac{1}{2}} \exp[-(TS-\overline{TS})^2/(2s^2)] \quad ,$$

where $\overline{TS}$ and s denote the respective mean and standard deviation.

Echo amplitude The two-target form is computed according to equation (6), where $\sigma=4\pi\, 10^{(TS/10)}$, and χ is uniformly distributed over π rad. That is,

$$f(\chi) = \pi^{-1} \quad ,$$

where $0 \leq \chi \leq \pi$.

Simulation of split-beam processing In addition to computing the sum beam for use with equation (6), the quadrant-beam responses are also computed. Half-beams are computed, assuming S=23.2, and the alongships and athwartships angles computed according to equation (10). Use of the resulting values in equation (11) determines the apparent single-target position (θ,ϕ), thence the sum-beam compensation factor b if within the limiting angle. For a single realization of the described stochastic model, then, the apparent backscattering cross section is

$$\hat{\sigma} = |b_1 \sigma_1^{\frac{1}{2}} + b_2 \sigma_2^{\frac{1}{2}} \exp(i\chi)|^2 / \hat{b}^2 \quad , \tag{12}$$

and corresponding apparent target strength is

$$\hat{TS} = 10 \log \frac{\hat{\sigma}}{4\pi} \quad . \tag{13}$$

Apparent target strength distribution Repeated exercise of the model determines a series of values for the apparent target strength. In this way the distribution f(TS) is generated. When simulated on a digital computer, the values are sorted in contiguous TS bins of width 0.5 dB.

Numerical parameters By simulation, two targets are allowed to occupy a range of paired positions entirely covering the transducer beam cross section with equal probability of occurrence. This is done by systematic and uniform variation of the polar angles θ_1 and θ_2 in 50 equal increments $\Delta\theta$ over 4.66 deg. The azimuth ϕ_1 is varied over the range $[0,\pi/4]$ in six increments $\Delta\phi_1=\pi/24$, and ϕ_2 is moved over the range $[\phi_1,\phi_1+\pi]$ in 16 increments of size $\Delta\phi_2=\pi/16$. The represented incremental area thus increases as $\sin\theta_1 \sin\theta_2\, \Delta\theta_1\, \Delta\theta_2\, \Delta\phi_1\, \Delta\phi_2$. The phase χ is varied uniformly over the range $[0,\pi]$ rad in 19 increments of size $\Delta\chi=\pi/19$. In the first case of constant target strengths, these are applied directly. In the second case of normally distributed target strengths, these are independently drawn from the same distribution for each combination of values θ_1, θ_2, ϕ_1, and ϕ_2. A pseudo-random number generator of linear conguential type is employed, with simple realization on FORTRAN compiler f77 as implemented on SUN computers.

RESULTS AND DISCUSSION

Apparent target strength distributions are shown in Fig. 2 for the case of constant target strengths and in Fig. 3 for the case of normally distributed target strengths.

In the case of the constant target strengths, shown in Fig. 2, the strongest effect is observed for equal target strengths, in Fig. 2a. With decreasing signal-to-noise ratio (SNR) in Figs. 2b-d, the effect of the second, weaker target strength is seen to be progressively less, evidently serving as a minor perturbation to the single-target distribution $f_1(TS)=\delta(TS)$. The results are further illustrated by the change in average backscattering cross section of the apparent single target. For the distributions shown in Figs. 2a-d, the corresponding logarithmic measure is 2.04, 0.91, 0.52, and 0.12 dB, respectively.

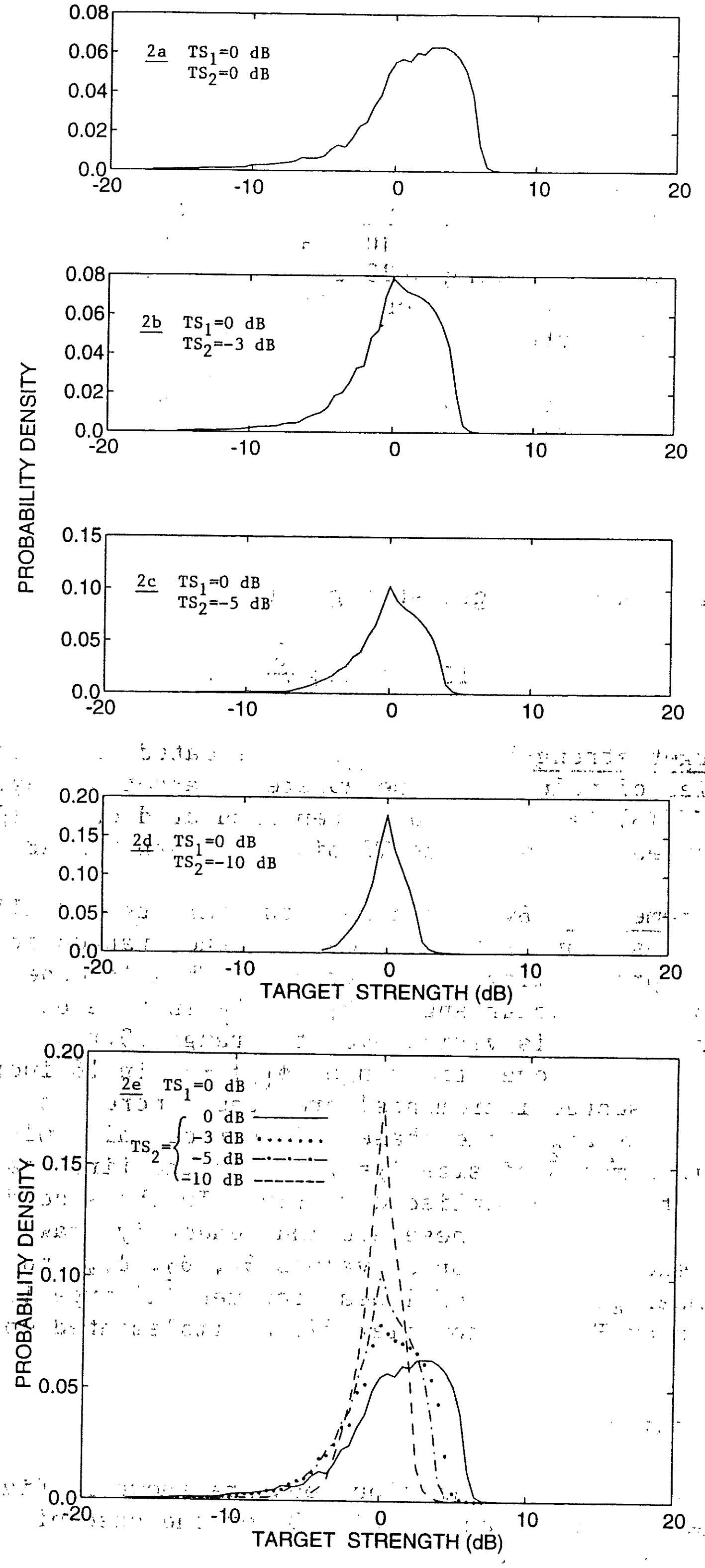

Fig. 2. Probability density functions of the apparent single-target target strength due to coincident echoes from two targets in the main beam of the SIMRAD ES38B split-beam transducer, with constant target strengths $TS_1=0$ dB and TS_2 as indicated in parts a-d. Part e is a synopsis of the four parts, but with same scale.

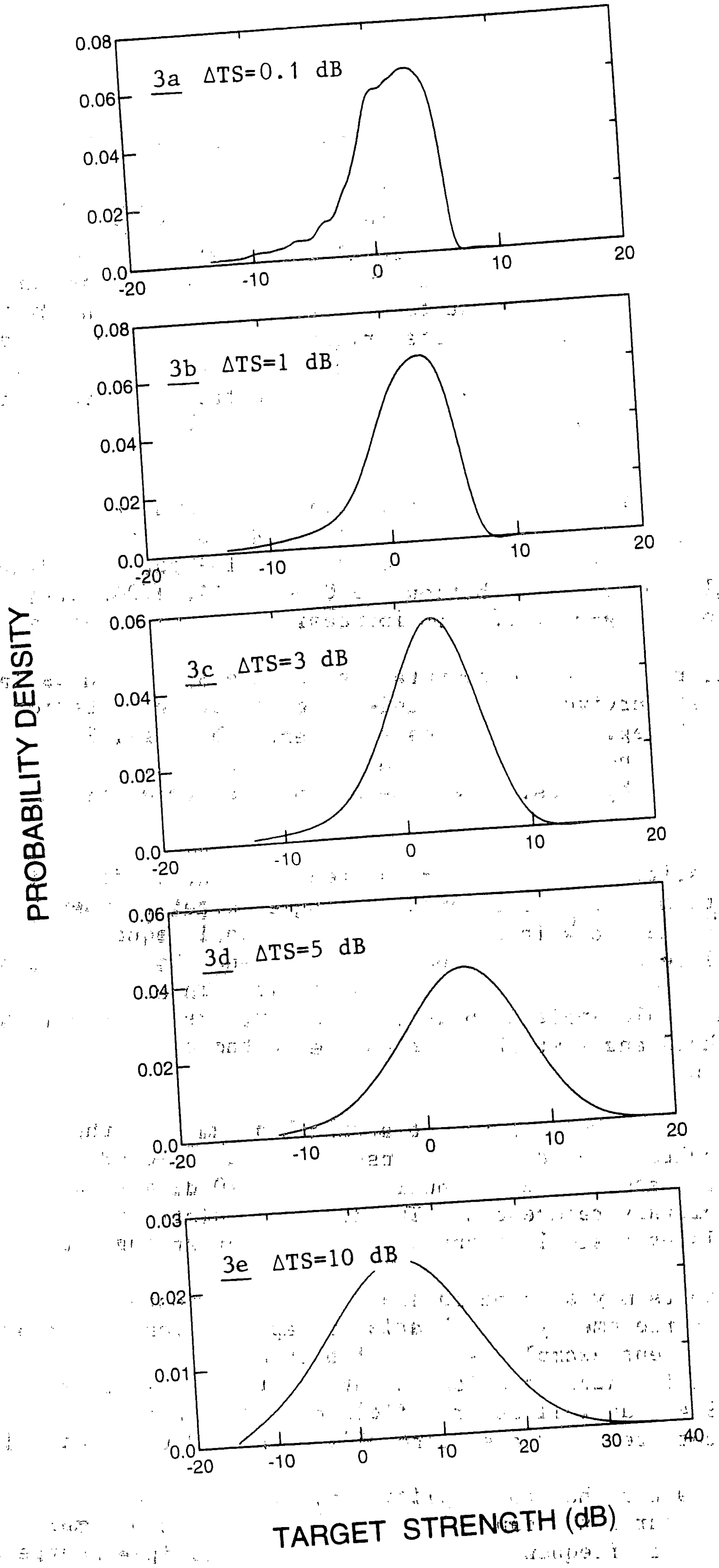

Fig. 3. Probability density function of the apparent single-target target strength due to coincident echoes from two targets in the main beam of the SIMRAD ES38B split-beam transducer, with target strengths independently drawn from the same normal distribution of target strength, N($\overline{TS}$,ΔTS), where TS=0 dB and ΔTS assumes the indicated values.

In the case of the normally distributed target strengths, the resultant distributions of apparent target strength in Fig. 3 display characteristics that are consistent with those in Fig. 2 and which can be understood in their light. Firstly, the distribution in Fig. 3a closely resembles that in Fig. 2a, as indeed it should since the case of constant and equal target strengths can be viewed as the limiting case of a normal distribution with vanishing standard deviation. Secondly, the distribution of apparent target strength due to the distribution N(0,10) bears a closer resemblance to its original distribution than do any of the others. With increasing dispersion, the chance of two values drawn from the same distribution being very similar is small, while that of being quite different is large, hence explaining the smaller effect, as also observed in Fig. 2d compared to that in Fig. 2a.

The mean values of the apparent distribution, as computed in the intensity or σ-domain, are 2.04, 5.12, 7.31, 9.45, and 15.33 dB for the five distributions arranged in order of increasing standard deviation. The corresponding values of the underlying single-target distribution are 0.00, 0.11, 1.00, 2.75, and 10.32 dB, as this distribution is log-normal, with increasing bias with increasing width.

The several distributions and computations of average measures include only those echoes that survive the detected-angle selection criterion, namely that θ not exceed 4.66 deg. In the cases represented by Figs. 2a-d, the percentage of accepted echoes is 77.9, 81.8, 83.6, and 86.8%, respectively. In the cases represented by Figs. 3a-e, the acceptance number is in the range 77.7-79.3%.

A detailed investigation, not otherwise reported here, identifies the nature of the rejection process for apparent single targets. When the quantities $b_1\sigma_1^{\frac{1}{2}}$ and $b_2\sigma_2^{\frac{1}{2}}$ in equation (6) are nearly equal, and the phase factor χ is close to π, the sum becomes small and the apparent phase angle unstable. Out-of-range values can then result. These are rejected if greater than the threshold angle 4.66 deg, but other, irregular values not exceeding the threshold angle wreak their damage on the apparent target strength distribution.

The particular mean levels of target strength assumed in the computations do not limit the results. In fact, the constant value TS_1=0 dB assumed in the computations in Fig. 2 and mean distribution value $\overline{TS}$=0 dB assumed for Fig. 3 may be viewed as arbitrary references. The displayed distributions apply to other absolute levels by a simple translation in target strength domain.

The present results may also be interesting in the context of baseline decorrelation and interferometry, which arise in applications of radar and sonar. A specific current example is that of bathymetry by side-scan sonar, for which baseline decorrelation may arise from two scatterers (Jin and Tang, MS 1994), as well as from field correlation or the result of a large number of scatterers, treated generally by Li and Goldstein (1990).

In general, no matter what the application, simultaneous multiple-frequency measurements can help resolve situations of ambiguity. The phase is sensitive to frequency, so situations of multiple scatterers will differentiate themselves from single-scatterer situations through frequency-dependent phases. If the apparent target position varies with frequency, it can be assumed to be due to the presence of multiple scatterers at similar range, hence can be rejected.

CONCLUSIONS

Clearly, the presence of multiple targets at similar range can change the character of a target strength distribution as determined with a split-beam echo sounder. Two consequences are broadening of the distribution and biasing of the average measure of target strength. The effect of digital signal processing on split-beam operation, not simulated here, is to produce a further, slight broadening of the distribution, but without significant bias.

While the present analysis aims to quantify the effects of coincidence in two-target echoes on target strengths, as derived with a particular split-beam target strength analyzer, the effects are recognized to be common to other methods of target strength determination that depend on the resolution of single targets. Avoidance of multiple-target effects by operating only under unambiguous conditions of dispersion is the recommended practice.

ACKNOWLEDGEMENTS

E. Ona is thanked for calling attention to the problem. Discussions with T. K. Stanton on the phenomenon of instability in detection angles of apparent single targets are gratefully acknowledged. D. Chu and D. Tang are thanked for information on wider applications of the work. Ø. Østensen is thanked for assistance in preparing Fig. 3, and N. Diner, for rendering the abstact.

REFERENCES

Bodholt, H. 1990. Split-beam transducer for target strength measurement. Contribution to the Scandinavian Cooperation Meeting in Acoustics, Ustaoset, Norway, January 1990. 20 pp. [mimeo.]

Bodholt, H., Nes, H., and Solli, H. 1989. A new echo-sounder system. Proc. IOA, 11(3): 123-130.

Ehrenberg, J. E. 1979. A comparative analysis of *in situ* methods for directly measuring the acoustic target strength of individual fish. IEEE J. Ocean. Eng., OE-4: 141-152.

Foote, K. G. 1991. Summary of methods for determining fish target strength at ultrasonic frequencies. ICES J. mar. Sci., 48: 211-217.

Jin, G., and Tang, D. MS 1994. Uncertainties in differential phase estimation with the Benthic Acoustic Measurement System.

Li, F. K., and Goldstein, R. M. 1990. Studies of multibaseline spaceborne interferometric synthetic aperture radars. IEEE Trans. Geoscience and Remote Sensing, 28: 88-97 (1990).

Mackenzie, K. V. 1981. Nine-term equation for sound speed in the oceans. J. acoust. Soc. Am., 70: 807-812.